eLIFE elifesciences.org

RESEARCH ARTICLE

Figures and figure supplements

Modulation of the *Erwinia* ligand-gated ion channel (ELIC) and the 5-HT_3 receptor via a common vestibule site

Marijke Brams *et al*

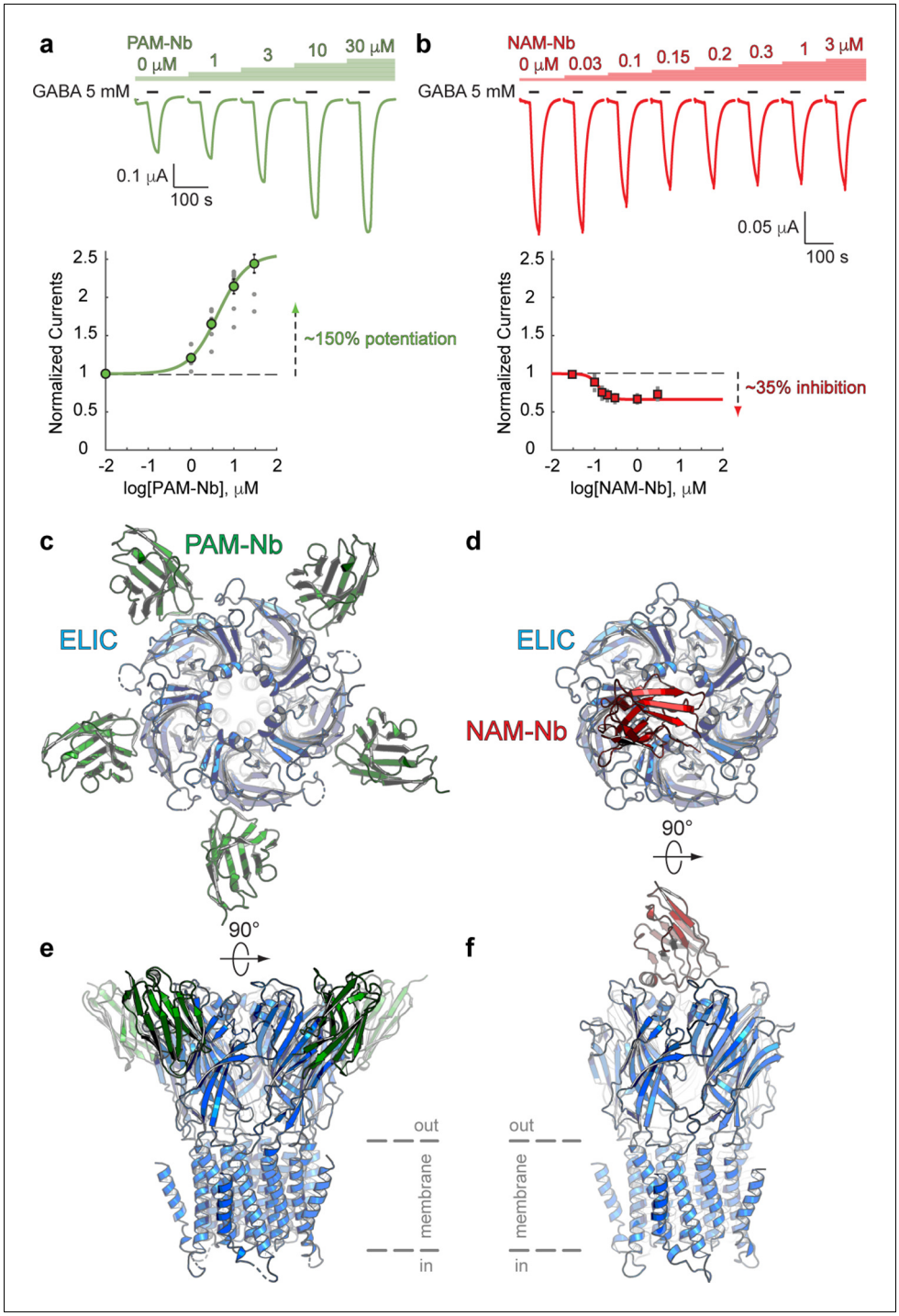

Figure 1. Nanobodies active as allosteric modulators and structures bound to the ELIC channel. (**a, b**) Electrophysiological recordings of ELIC activated by the agonist GABA and in the presence of increasing concentrations of PAM-Nb (a, green) or NAM-Nb (b, red). The curve represents a fit to the Hill equation to the normalized current responses. Circles represent averaged data with standard errors. (**c,d**) X-ray crystal structures of ELIC bound by PAM-Nb (**c**) or NAM-Nb (**d**). The cartoon representation shows a top-down view onto the ELIC pentamer along the fivefold axis (blue). (**e,f**) Side views from **c,d**). The dashed lines indicate the presumed location of the membrane boundaries.

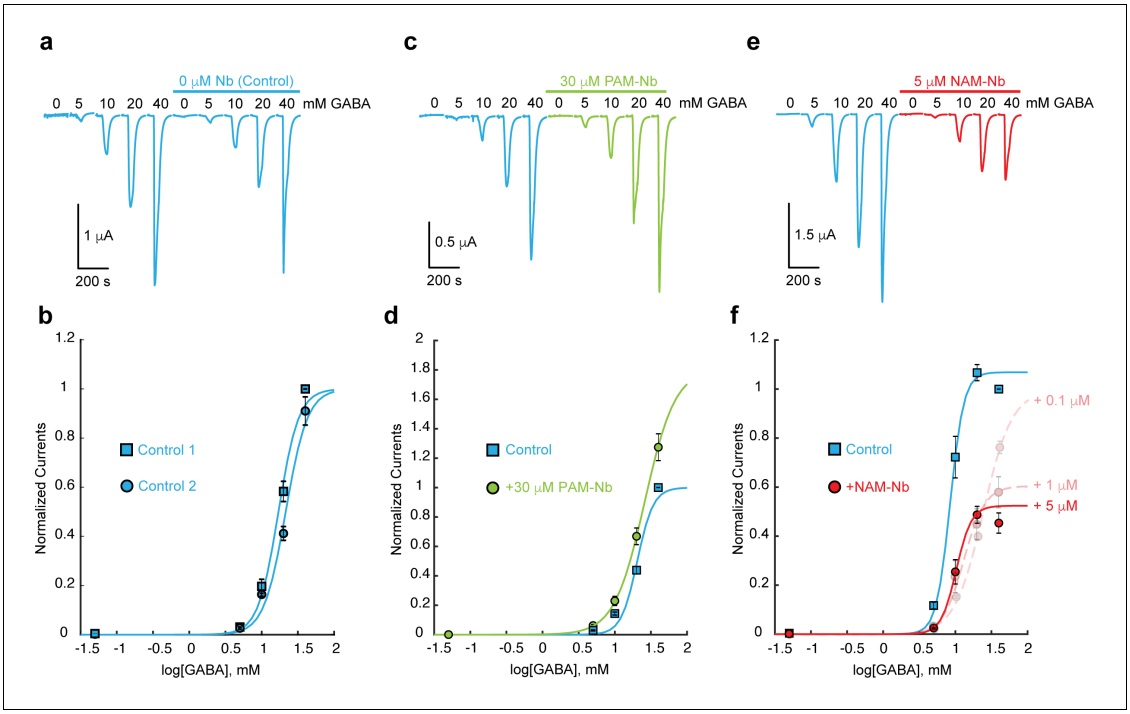

Figure 1—figure supplement 1. The effect of PAM-Nb and NAM-Nb on the GABA concentration-activation curve. (**a**) An example control experiment with two consecutive applications of a series of GABA concentrations (5–40 mM). ELIC is prone to desensitization, but this effect can be minimized by excluding GABA concentrations > 40 mM. (**b**) Concentration-response curves for three such experiments are similar. (**c,d**) 30 μM PAM-Nb shows potentiation at all GABA concentrations (example traces in **c**), consistent with a leftward shift of the concentration-activation curve and/or increase of the maximal current (curves in **d**), n = 3). By excluding saturating concentrations of GABA we cannot accurately calculate EC_{50}-values, but we can determine nanobody potentiation or inhibition at each GABA concentration under conditions with minimal channel desensitization. Here, currents in the presence and absence of 30 μM PAM-Nb were significantly different (t-test) with p-values of 0.0081 (5 mM), 0.0495 (10 mM), 0.0193 (20 mM) and 0.0455 (40 mM) (n = 3). Under control conditions p-values were 0.0012 (5 mM), 0.0013 (10 mM), <0.0001 (20 mM) and <0.0001 (40 mM) (n = 3). (**e,f**) Increasing concentrations of NAM-Nb (0.1, 1, 5 μM, example traces in **e**) show inhibition at all GABA concentrations, consistent with a rightward shift of the concentration-activation curve and/or decrease of the maximal current (curves in **f**), n = 5). Currents in the presence and absence of 5 mM NAM-Nb were significantly different (t-test) with p-values of 0.0012 (5 mM), 0.0013 (10 mM), <0.0001 (20 mM) and <0.0001 (40 mM) (n = 5).

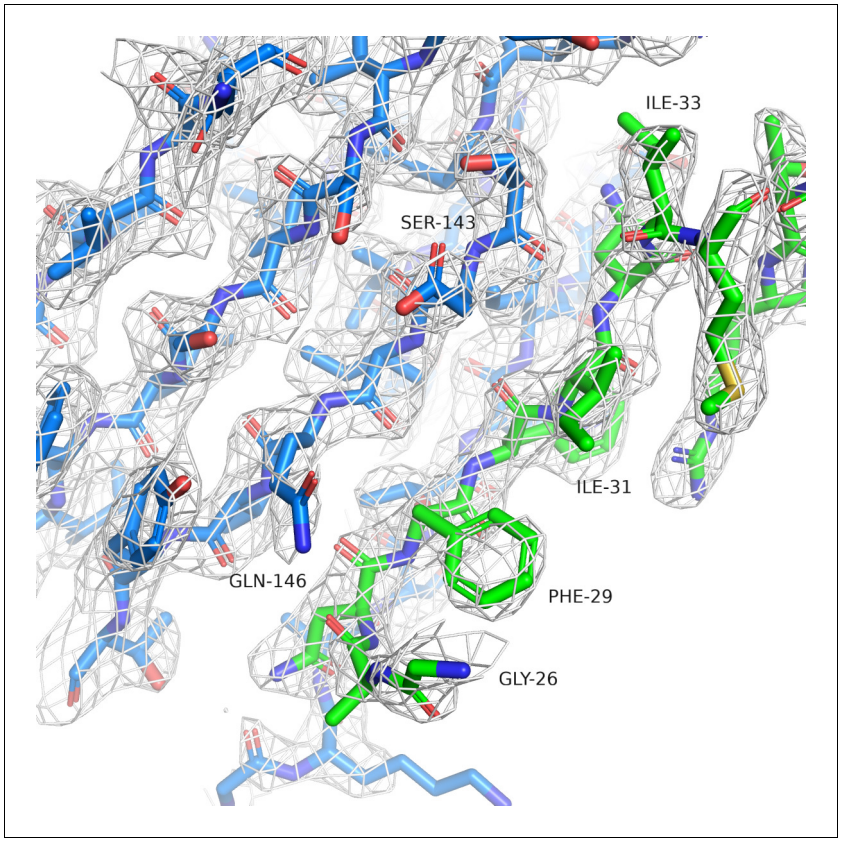

Figure 1—figure supplement 2. Simulated annealing omit map for PAM-Nb ELIC structure. The white mesh shows a simulated annealing omit map calculated in PHENIX and contoured at a sigma level of 1.0 around a 12 Å sphere zoom of the ELIC-Nb interface. In the omit calculation an omit box around the entire chain F (green) of the PAM-Nb was selected. ELIC is shown in blue and selected residues of the interaction interface are indicated.

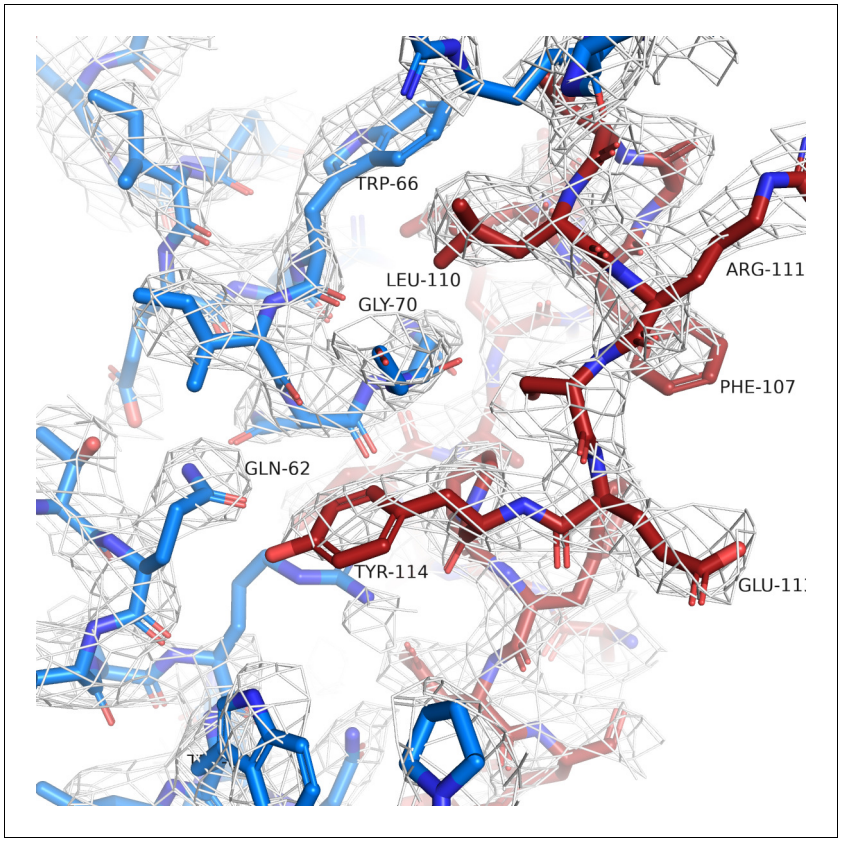

Figure 1—figure supplement 3. Simulated annealing omit map for NAM-Nb ELIC structure. The white mesh shows a simulated annealing omit map calculated in PHENIX and contoured at a sigma level of 1.0 around a 12 Å sphere zoom of the ELIC-Nb interface. In the omit calculation, an omit box around the entire chain K (red) of the PAM-Nb was selected. ELIC is shown in blue and selected residues of the interaction interface are indicated.

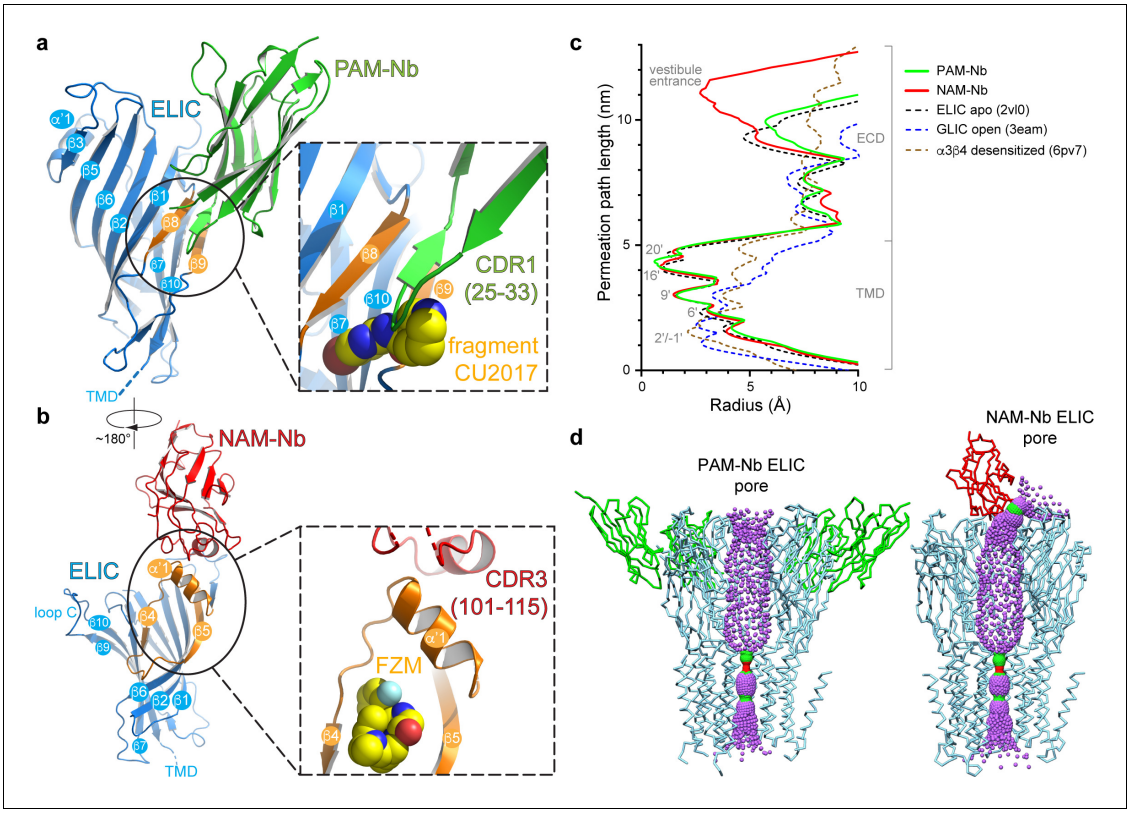

Figure 2. Detailed nanobody interaction sites in ELIC and channel pore analysis. (**a**) A detailed view of the interaction between PAM-Nb (green) and a single ELIC subunit (blue). The binding site for PAM-Nb overlaps with a known allosteric binding site, in a related pLGIC, for a small molecule fragment called CU2017, shown as spheres (carbon yellow, nitrogen blue) (***Delbart et al., 2018***; pdb code 5oui). (**b**) Detailed view of the interaction between NAM-Nb (red) and a single ELIC subunit (blue). The binding site for NAM-Nb involves a region which borders a known allosteric binding site for flurazepam in ELIC (***Spurny et al., 2012***; pdb code 2yoe). (**c,d**) Analysis of the ELIC channel pore radius for PAM-Nb, NAM-Nb bound structures and references structures.

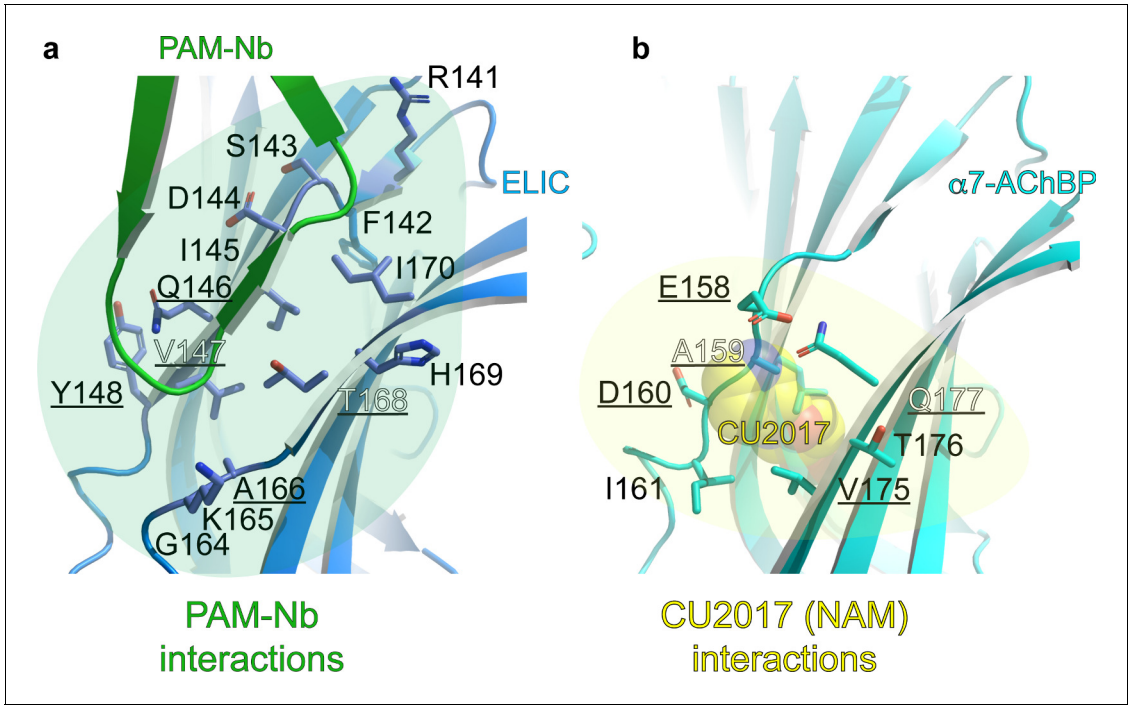

Figure 2—figure supplement 1. Detailed atomic interactions between PAM-Nb and ELIC, compared to those between CU2017 (a NAM molecule) and α7-AChBP (***Delbart et al., 2018***). (**a–b**) The cartoon shows that the binding site of the PAM-Nb (green) in ELIC (blue) (**a**) is homologous to the CU2017 (yellow spheres) site in α7-AChBP (cyan) (**b**). For clarity, only residues at the receptor site are shown as sticks. Residues that are commonly targeted in both structures are underlined: Q146, V147, Y148 (in ELIC) corresponds to E158, A159, D160 (in α7-AChBP) and A166, T168 (in ELIC) corresponds to V175, Q177 (in α7-AChBP). ELIC residues involved in unique interactions with PAM-Nb are: R141, F142, S143, D144, I145, G164, K165, H169, I170 and these could possibly mediate *positive* allosteric modulation. α7-AChBP residues involved in unique interactions with NAM-Nb are: I161 and T176, and these could possibly mediate *negative* allosteric modulation. See ***Figure 2—figure supplement 1—source data 1*** for list of detailed atomic interactions. 3.8 Å was used as a distance cutoff for interactions. H-bond interactions are shown in bold in the associated source file.

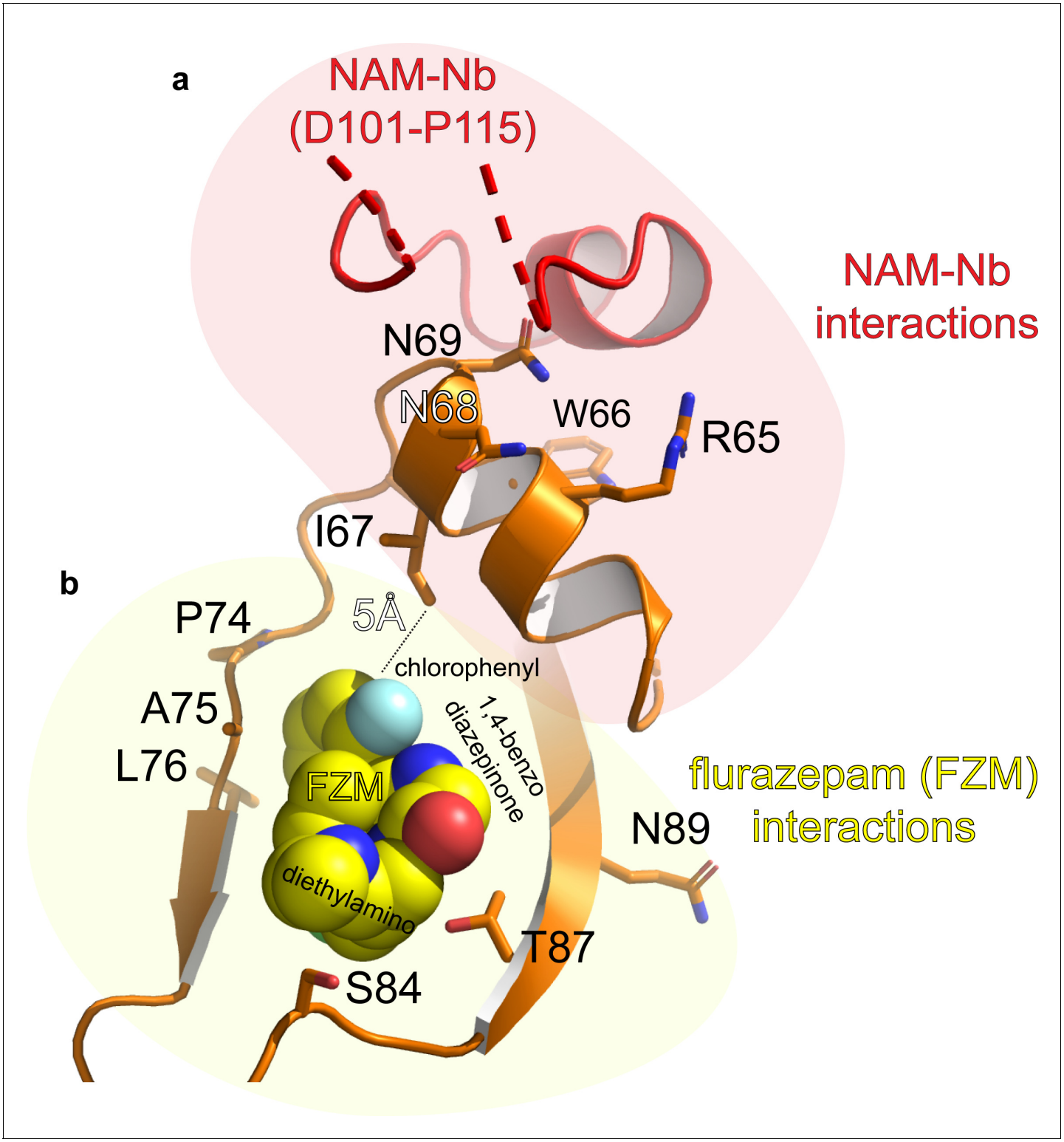

Figure 2—figure supplement 2. Detailed atomic interactions between NAM-Nb and ELIC, compared to those between flurazepam (a PAM molecule) and ELIC (***Spurny et al., 2012***). (**a**) The cartoon shows that the binding site of the NAM-Nb (red) is adjacent to the flurazepam site (yellow spheres) in the vestibule of ELIC (orange). For clarity, only residues at the receptor site are shown as orange sticks. (**b**) See ***Figure 2—figure supplement 2—source data 1*** for list of detailed atomic interactions. 3.8 Å was used as a distance cutoff for interactions. H-bonds and electrostatic interactions are shown in bold in the associated source file. The residues in the α'1-helix in ELIC (R65–N69) could be involved in *negative* allosteric modulation whereas P74-N89 in ELIC could be involved in *positive* allosteric modulation.

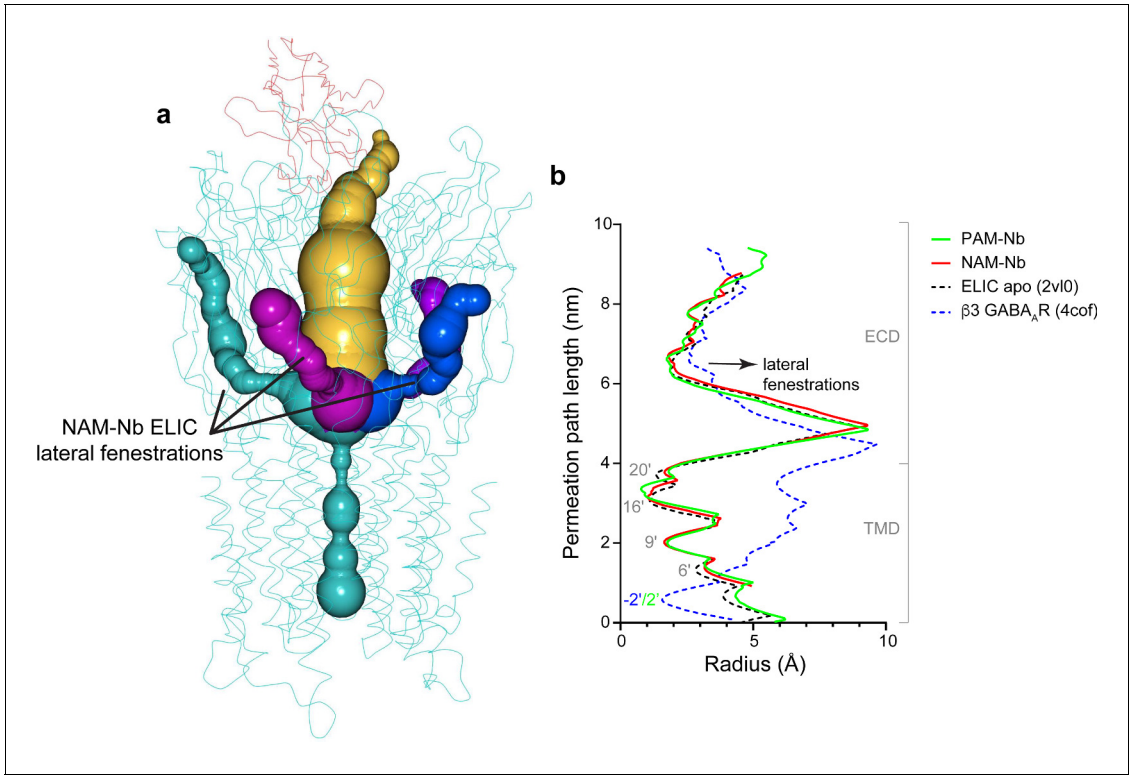

Figure 2—figure supplement 3. Analysis of pore radius profiles through lateral fenestrations located at subunit interfaces in ELIC and the β3 GABA$_A$R (***Miller and Aricescu, 2014***). (**a**) Pore radius profiles extending into lateral fenestrations (green, magenta, blue) at subunit interfaces or the extracellular vestibule entrance (amber) in the NAM-Nb bound structure. (**b**) Pore radius plotted along the permeation path and compared for ELIC apo (black), PAM-Nb bound ELIC structure (green), NAM-Nb bound ELIC structure (red) and β3 GABA$_A$R (blue).

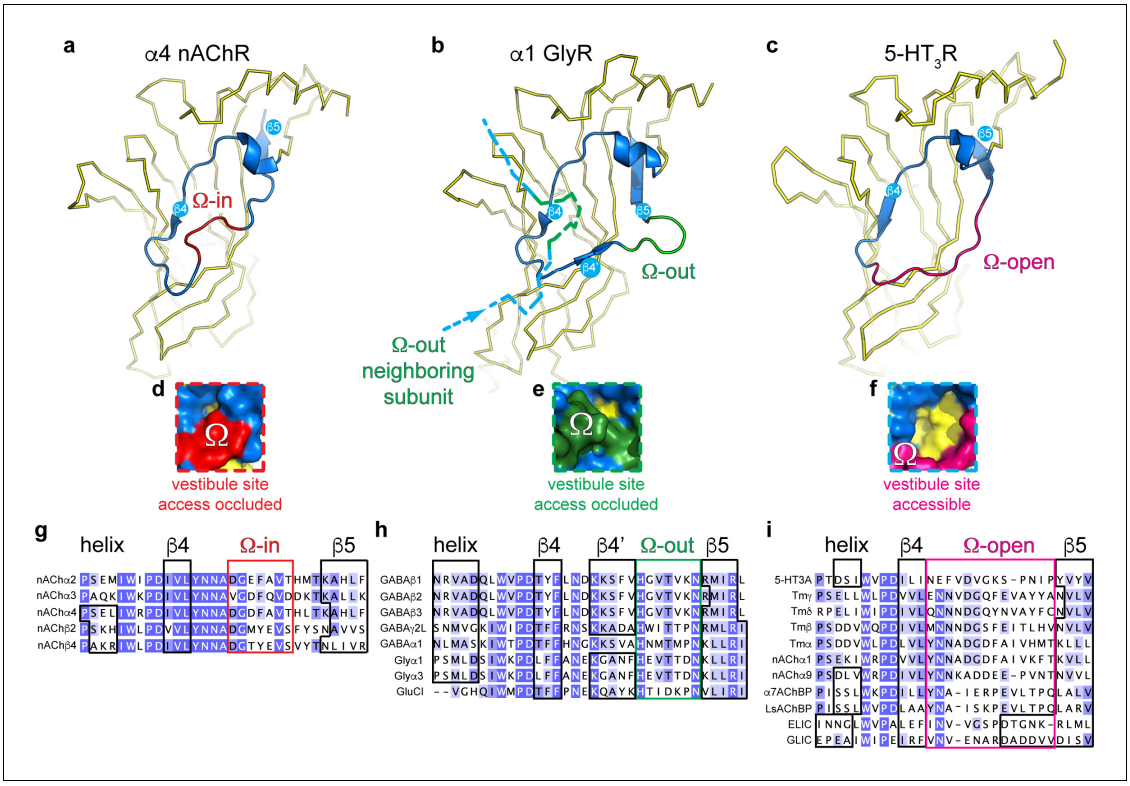

Figure 3. Distinct conformations of the vestibule site in pentameric ligand-gated ion channels. (**a–c**) Yellow ribbon representation of a single subunit ligand binding domain. Part of the vestibule site (shown in blue cartoon), called the Ω-loop, adopts three distinct conformations in different pLGICs: the Ω-in (red, (**a**), Ω-out (green, (**b**) and Ω-open conformation (magenta, (**c**). (**d-f**) Insets show a zoom of the Ω-loop in surface representation to illustrate occluded vestibule site access in the Ω-in and Ω-out conformations, compared to an accessible vestibule site in the Ω-open conformation. (**g–i**). Sequence alignment of the Ω-loop and neighboring residues in pLGICs for which structures have been elucidated.

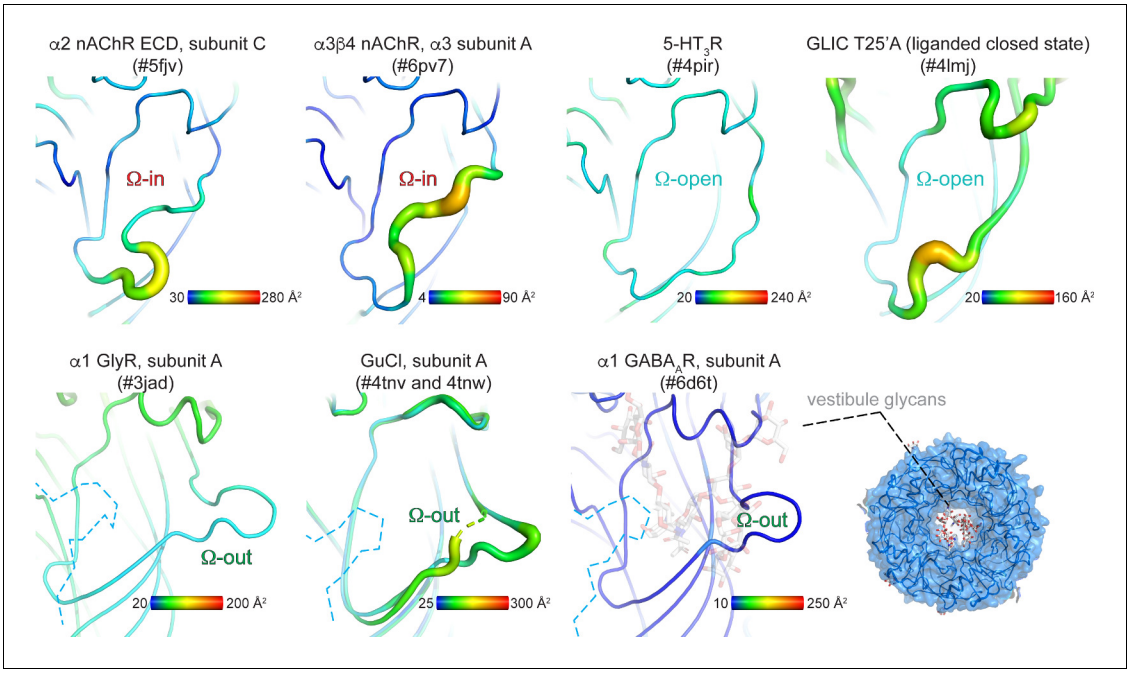

Figure 3—figure supplement 1. B-factor analysis of the Ω-loop compared to other regions within each structure. The vestibule site is depicted in the 'putty' cartoon presentation. Yellow-red regions indicate example structures with higher average B-factors per residue compared to cyan-blue regions. B-factors are an indicator of vibrational movement. Enhanced B-factors were not identified in any 5-HT_3R (Ω-open), GlyR (Ω-out) or $GABA_A$R (Ω-out) structures determined to date. In $GABA_A$R structures the vestibule access is additionally restricted by N-linked glycans.

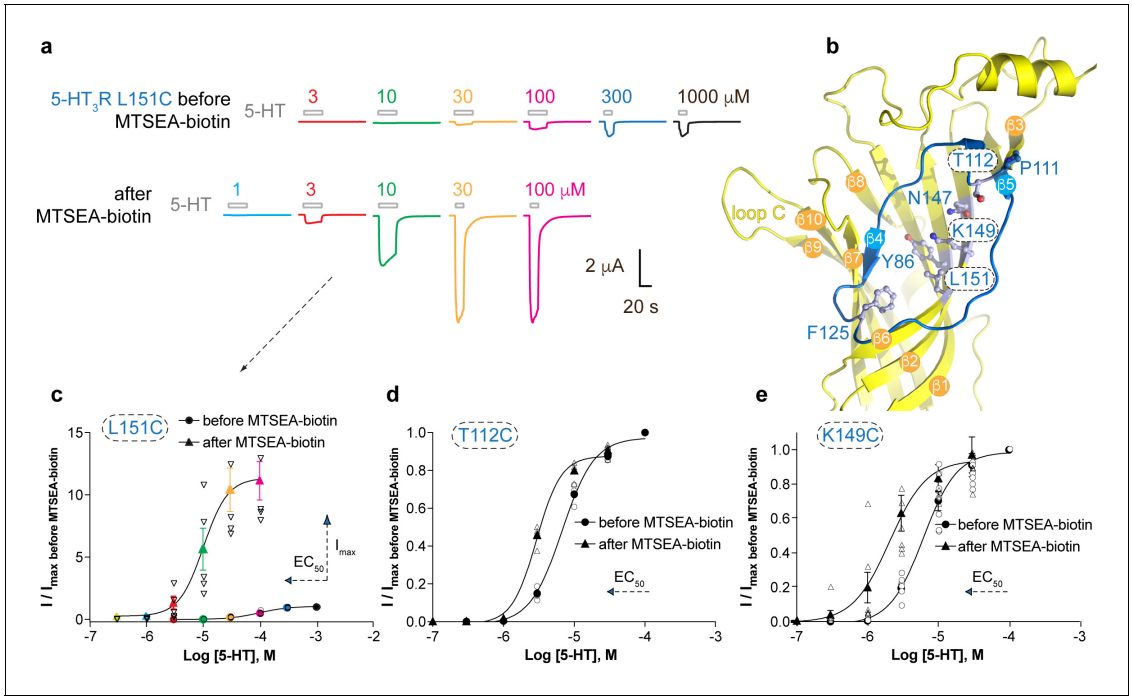

Figure 4. Allosteric modulation of the 5-HT_3A receptor through chemical modification of engineered cysteines in the vestibule site. (**a**) Example traces of agonist-evoked channel responses of the L151C 5-HT_{3A}R mutant before and after modification with MTSEA-biotin show potentiation after cysteine modification. (**b**) Location of L151C and other engineered cysteine mutants in this study, shown in ball and stick representation. (**c**) Concentration-activation curves before and after modification with MTSEA-biotin are a Hill curve fit for the recordings shown in (**a**) as well as additional data for T112C (**d**) and K149C. (**c–e**) Each of these three mutants reveal a leftward shift of the curve upon cysteine modification, consistent with a positive allosteric effect. In the case of L151C, this effect is combined with a large increase of the maximal current response.